EASR

Engineering and Applied Science Research

https://www.tci-thaijo.org/index.php/easr/index

Published by the Faculty of Engineering, Khon Kaen University, Thailand

Follow-up study of aircraft parameter estimation for lateral dynamics using self-adaptive teaching-learning based optimization with acceptance probability

Yodsadej Kanokmedhakul*[1)] and Nantiwat Pholdee[2, 3)]

[1)]Department of Mechanical Engineering, Faculty of Engineering, Mahidol University, Nakhon Pathom, Thailand
[2)]Sustainable Infrastructure Research and Development Center, Khon Kaen University, Khon Kaen, Thailand
[3)]Department of Mechanical Engineering, Faculty of Engineering, Khon Kaen University, Khon Kaen, Thailand

Received 23 July 2024
Revised 19 February 2025
Accepted 11 March 2025

Abstract

This paper is a follow-up on using self-adaptive teaching-learning based optimization with an acceptance probability (SATLBO-AP), tailored specifically for aircraft parameter estimation, and extended to aircraft lateral dynamics, previously tested for aircraft longitudinal dynamics. The lateral dynamic is more complicated than the longitudinal with additional parameters, input and output. Since the problem has changed, the performance of SATLABO-AP requires reevaluation. Thus, a comparison between newly developed algorithms and recently proposed algorithms is conducted. The problem setup is carried out in a way similar to earlier work, but with a lateral dynamic. The results show that SATLBO-AP outperforms other algorithms in terms of convergence and consistency regarding noise level added to the validation signal.

Keyword: Aircraft parameter estimation, Aircraft lateral dynamics, System identification, Evolutionary algorithm, Self-adaptive algorithm

Nomenclature

C_Y, C_l, C_n	Coefficient of lateral, coefficient of rolling and coefficient of yawing moment
C_{Y_0}, C_{l_0}, C_{n_0}	Trim parameter
p, q, r	Angular velocity of roll, pitch and yaw
ϕ, θ, ψ	Roll, pitch and yaw angle
u, v, w	Airspeed component of x, y and z axis
I_x, I_y, I_z	Moment of inertia about x, y and z axes
Θ	Vector of unknown parameters
α	Angle of attack
β	Side slip angle
$C_{Y_\beta}, C_{Y_p}, C_{Y_r}, C_{Y_{\delta r}}$	$\partial C_Y/\partial\beta$, $\partial C_Y/\partial(pb/2u_0)$, $\partial C_Y/\partial(rb/2u_0)$, $\partial C_Y/\partial\delta r$ respectively
$C_{l_\beta}, C_{l_p}, C_{l_r}, C_{l_{\delta a}}, C_{l_{\delta r}}$	$\partial C_l/\partial\beta$, $\partial C_l/\partial(pb/2u_0)$, $\partial C_l/\partial(rb/2u_0)$, $\partial C_l/\partial\delta a$, $\partial C_l/\partial\delta r$ respectively
$C_{n_\beta}, C_{n_p}, C_{n_r}, C_{n_{\delta r}}$	$\partial C_n/\partial\beta$, $\partial C_n/\partial(pb/2u_0)$, $\partial C_n/\partial(rb/2u_0)$, $\partial C_n/\partial\delta r$ respectively
$\bar{q}$	Dynamic pressure

1. Introduction

In the control industry, a mathematical model is a crucial part for performing model analysis and control design; without it this task would be much more difficult. The model needs to represent the real-world hardware sufficiently well to command the system as designed especially for the aircraft. Aircraft control design is very challenging due to the vast flight envelope, while the state of the aircraft is continuously changing. Typically, the mathematical model of an aircraft is constructed using aerodynamic parameters, including stability and control derivatives. These parameters are evaluated from empirical models [1], numerical models (a vortex lattice method) [2], computational fluid dynamics (CFD) [3] and wind tunnel tests. However, the aircraft may deviate from its mathematical models due to the manufacturing processes, environmental factors, and even simplification of the mathematical model itself. Through the system identification, the system model can be obtained from flight tests and can be useful for validation purposes.

System identification is a process of finding a mathematical model using only input and output data from the physical system. It is helpful when the model is unknown. In aircraft, the model equation is known, so it is categorized as parameter estimation instead. The technique of parameter estimation is widely used in the aircraft industry, and consists of the Equation Error Method (EEM) [4-7], the Output Error Method (OEM) [8-10], and the Filter Error Method (FEM) [11-14]. These methods are very powerful, but require a good initial solution to perform the search; the initial guess relies on trial and error. A bad initial guess consequently leads to convergence

*Corresponding author.
Email address: yodsadej.kan@mahidol.ac.th
doi: 10.14456/easr.2025.22

to a local optimum point or even a nonconvergent solution. Thus, the development of the technique has continued, artificial intelligence [15-19] and even meta-heuristics (MH) have been successfully deployed. The advantage of the MH approach over artificial intelligence is that MH does not involve training the model before employment.

MH, classified as a nonlinear optimization approach, is being deployed successfully across various engineering fields. The application of MH to parameter estimation is seen in biological systems [20], wind and energy [21], induction motors [22], etc. Nevertheless, the MH employed in these topics is very limited; there are still plenty of MH applications to be explored. Furthermore, using MH for aircraft parameter estimation has rarely been done in the aircraft industry, and thus a study of this topic is beneficial.

Although MH does not need a good initial guess, its consistency and performance depend on the problem. Teaching-learning based optimization (TLBO) [23] is chosen as a baseline algorithm for improvement, due to its capability of solving the inverse problem [24]. It has been developed to solve parameter estimation for photovoltaic models as improved teaching-learning based optimization (ITLBO) [25], which modifies both teaching and learning phases, avoiding the local minimum-points that parameter estimation problems usually struggle with. Improvement on TLBO for aircraft parameter estimation in the longitudinal model has also been carried out, leading to Self-Adaptive Teaching-Learning Based Optimization with an Acceptance Probability (SaTLBO-AP) [26]. The concept of acceptance probability prevents the solution from converting to a single optimum point at the early stage of the optimization, and allows the population to converge to the optimum point near the end of the optimization run. While SaTLBO-AP performs very well on longitudinal problems, lateral dynamics on the other hand needed to be tested. Lateral dynamics is more complex than longitudinal; in longitudinal motion, the aircraft's movement is primarily constrained to the pitch axis. In contrast, lateral dynamics involve a coupling between the roll and yaw axes. Furthermore, the aircraft's behavior is influenced by additional control surfaces and rudder ailerons. As a result, there are additional aerodynamic coefficients, more control signals, and consequently, a more complex output response. Thus, a comparison to recently developed MH is required. This paper is a continuation of previous work [26] using the HANSA-3 aircraft to construct the inverse optimization problem [19]. Then we perform SATLBO-AP on lateral dynamics comparing 15 MHs, consisting of Ant Lion Optimizer (ALO) [27], Dragonfly Algorithm (DA) [28], Grasshopper Optimization Algorithm (GOA) [29], Grey Wolf Optimization (GWO) [30], Moth-Flame Optimization (MFO) [31], Muti-Verse Optimizer (MVO) [32], A Sine Cosine Algorithm (SCA) [33], Salp Swarm Algorithm (SSA) [34], Water Cycle Algorithm (WCA) [35], Whale Optimization Algorithm (WOA) [36], Self-Adaptive Differential Evolution Algorithm (SaDE) [37], Improved Multi-Operator Differential Evolution (IMODE) [38], TLBO [23] and ITLBO [25]. The results are subsequently analyzed and discussed.

2. Problem formulation

The conventional aircraft dynamic can be determined by the second law of Newton. The aircraft are assumed to be rigid bodies, which furthermore simplifies the equation. The equation is a line around the north-east down system consisting of translation and rotation of these 3 axes with a total of 6 degrees of freedom. These sets of equations are then divided into longitudinal and lateral motion; these 2 dynamics have little effect on each other, so are usually separated for easier operation whether tuning or, in this paper, identifying parameters. This work will focus only on the lateral dynamics and parameters of the aircraft. The lateral motion considers only the translation on the y axis and rotation of x and z axis with a total of 3 degrees of freedom. The lateral motion of the aircraft can be described by a set of dimensionless aerodynamic coefficients, which in this study uses the HANSA-3 aircraft model. These non-aerodynamic coefficients can be derived from the geometry of the aircraft. Eqs.1-3 are combined force and moment coefficients from the influence of the state of the aircraft in lateral dynamics.

$$C_Y = C_{Y_0} + C_{Y_\beta}\beta + C_{Y_p}(\frac{pb}{2V}) + C_{Y_r}(\frac{rb}{2V}) + C_{Y_{\delta_r}}\delta_r \quad \text{Eq.1}$$

$$C_l = C_{l_0} + C_{l_\beta}\beta + C_{l_p}(\frac{pb}{2V}) + C_{l_r}(\frac{rb}{2V}) + C_{l_{\delta_a}}\delta_a + C_{l_{\delta_r}}\delta_r \quad \text{Eq.2}$$

$$C_n = C_{n_0} + C_{n_\beta}\beta + C_{n_p}(\frac{pb}{2V}) + C_{n_r}(\frac{rb}{2V}) + C_{n_{\delta_r}}\delta_r \quad \text{Eq.3}$$

The total force and moment can then be translated to the equation of motion of the aircraft in lateral dynamics comprising Eqs.4-10 with a total of 6 states.

$$\dot{\beta} = -r + \frac{gsin(\phi)}{V} + \frac{\bar{q}S}{mV}C_Y \quad \text{Eq.4}$$

$$C_1 = \bar{q}SbC_l \quad \text{Eq.5}$$
$$C_2 = \bar{q}SbC_n$$

$$\dot{p} = \frac{C_1 I_z + C_2 I_{xz}}{I_x I_z - {I_{xz}}^2} \quad \text{Eq.6}$$

$$\dot{r} = \frac{C_1 I_{xz} + C_2 I_x}{I_x I_z - {I_{xz}}^2} \quad \text{Eq.7}$$

$$\dot{\phi} = p \quad \text{Eq.8}$$

$$\dot{v} = -rV + \frac{\bar{q}S}{m}C_Y + gsin(\phi) \quad \text{Eq.9}$$

$$\dot{\psi} = psin(\phi) + rcos(\phi) \quad \text{Eq.10}$$

This study used the HANSA-3 aircraft lateral coefficients as a reference to perform parameter estimation with a total of 16 parameters. The unknown parameter vector can be expressed as

$$\boldsymbol{\Theta} = [C_{Y_0}, C_{Y_\beta}, C_{Y_p}, C_{Y_r}, C_{Y_{\delta_r}}, C_{l_0}, C_{l_\beta}, C_{l_p}, C_{l_r}, C_{l_{\delta_a}}, C_{l_{\delta_r}}, C_{n_0}, C_{n_\beta}, C_{n_p}, C_{n_r}, C_{n_{\delta_r}}]$$

These parameters are used in the aircraft lateral equation of motion Eq.1-10, and the flight conditions in Table 1 to simulate the behavior of the aircraft. The results of the simulation are seen in Figure 1 using 3-2-1-1 inputs of aileron and rudder leading to 6 outputs consisting of sideslip, roll rate, yaw rate, roll angle, velocity in the y-axis, and yaw angle. The output was later used as validation data in parameter estimation. The simulation is executed with a timestep of 0.025 seconds.

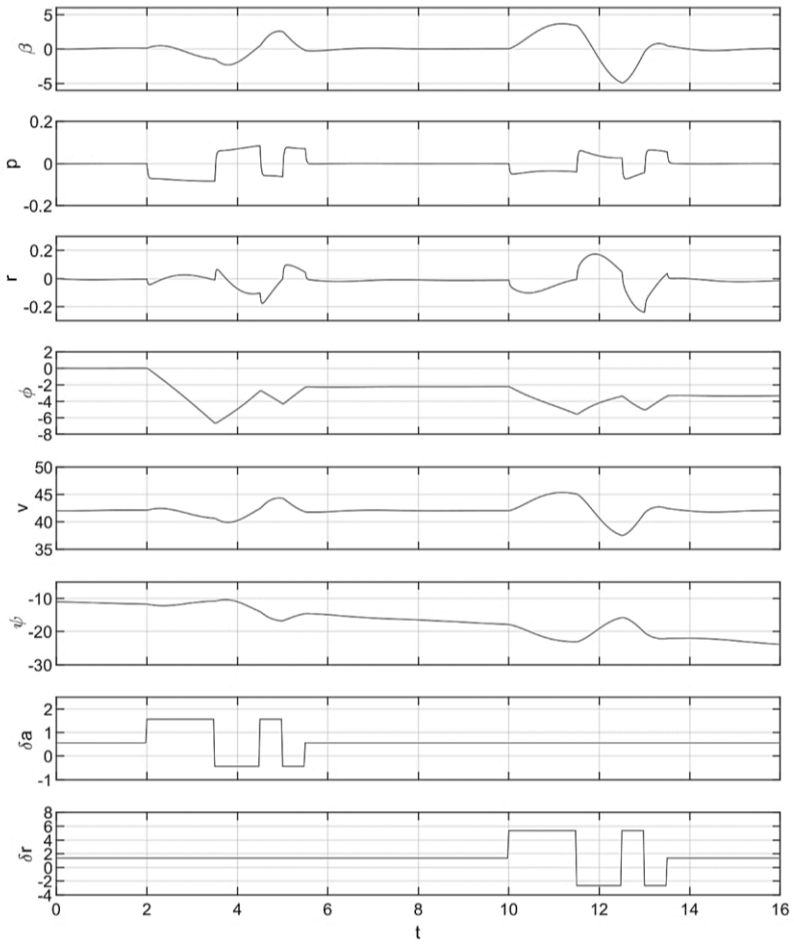

Figure 1 Lateral parameters simulated with 3-2-1-1 aileron and rudder

Table 1 Flight conditions and HANSA-3 properties

Variable	Value
Mean Aerodynamic Chord ($\bar{c}$)	1.21 m
Wingspan (b)	10.84 m
Reference Wing Area (S)	12.47 m^2
Mass (m)	758 kg
True Air speed (V)	52 m/s
Moment of Inertia (I_x)	873 $kg\ m^2$
Moment of Inertia (I_z)	1680 $kg\ m^2$
Moment of Inertia (I_{xz})	1144 $kg\ m^2$

3. The optimization problem

The optimization problem can be formed simply by minimizing errors between the lateral response of the actual data and the calculated response from the lateral coefficient. As there are several types of physical parameters with totally different units e.g. aircraft velocity and angular position, each estimation error is therefore normalized and then summed up. This step can be easily achieved by dividing by the absolute value of each state's real response expressed as:

$$\min: f(\boldsymbol{x}) = \sum_{i=1}^{l} \sum_{t=t_0}^{t_{end}} \frac{|\boldsymbol{r}_{real,i}(t) - \boldsymbol{r}_{estimate,i}(t)|}{|\boldsymbol{r}_{real,i}(t)|} \quad \text{Eq.11}$$

Subject to

$$\boldsymbol{L}_b \leq \boldsymbol{x} \leq \boldsymbol{U}_b$$

where design variables $\boldsymbol{x} = \boldsymbol{\Theta}$ are the target value of aerodynamic parameters $\left\{C_{D0}, C_{D\alpha}, C_{D_{\delta e}}, C_{L_0}, C_{L_\alpha}, C_{L_q}, C_{L_{\delta e}}, C_{m_0}, C_{m_\alpha}, C_{m_{q'}} C_{m_{\delta e}}\right\}$ subject to only lower ($\boldsymbol{L}_b$) and upper ($\boldsymbol{U}_b$) bound constraints. The details of the boundaries are shown in Table 2. The parameters $\boldsymbol{r}_{real,i}$ and $\boldsymbol{r}_{estimate,i}$ are respectively the i^{th} real and estimated lateral motion dynamics responses, whereas l is the number of lateral dynamics considered. The state and time response of the lateral motion $\boldsymbol{r} = \{\beta, p, r, \phi, \mathrm{v}, \psi\}^T$ can be numerically solved based on Eq. 12, while $\dot{\boldsymbol{r}}$ can be calculated based on Eqs. 1-10. The parameters t_0 and t_{end} are the initial and final times of simulation respectively. The state time-response used as real flight data is shown in Figure 1.

$$\boldsymbol{r}(t + \Delta t) = \boldsymbol{r}(t) + \int_t^{t+\Delta t} \dot{\boldsymbol{r}}(t)dt \qquad \text{Eq. 12}$$

Table 2 Lateral parameters of HANSA-3

Parameter	Real coefficient	L_b	U_b
C_{Y_0}	-0.013	-0.1	0.1
C_{Y_β}	-0.531	-10	0
C_{Y_p}	0.1	0	10
C_{Y_r}	0.7	0	10
$C_{Y_{\delta_r}}$	0.15	0	10
C_{l_0}	0.0015	-0.1	0.1
C_{l_β}	-0.031	-1	0
C_{l_p}	-0.27	-10	0
C_{l_r}	0.05	0	1
$C_{l_{\delta_a}}$	-0.153	-10	0
$C_{l_{\delta_r}}$	0.005	0	1
C_{n_0}	0.001	-0.1	0.1
C_{n_β}	0.061	0	1
C_{n_p}	-0.11	-10	0
C_{n_r}	-0.11	-10	0
$C_{n_{\delta_r}}$	-0.049	-1	0

4. Self-adaptive teaching-learning based optimization with an acceptance probability

A TLBO is one of the best algorithms for solving inverse problems [39-41], thus modification of the TLBO base algorithm is very appealing. The TLBO procedure consists of population initialization, reproduction and selection. In reproduction it has 2 phases, teaching and learning phases. More details on TLBO can be found elsewhere [23]. The teaching and learning phases are shown in Eqs.13 and 14.

$$\boldsymbol{x}^i_{teaching} = \boldsymbol{x}^i + rand\{\boldsymbol{x}_{teacher} - (T_F \boldsymbol{x}_{mean})\} \qquad \text{Eq. 13}$$

The offspring and parents are then put together, with the best of them being selected and sent to the learner phase. In the learner reproduction phase, a particular offspring can be created as:

$$\boldsymbol{x}^i_{learner} = \begin{cases} \boldsymbol{x}^i + rand(\boldsymbol{x}_{i1} - \boldsymbol{x}_{i2}) & if\ f(\boldsymbol{x}_{i1}) < f(\boldsymbol{x}_{i2}) \\ \boldsymbol{x}^i + rand(\boldsymbol{x}_{i2} - \boldsymbol{x}_{i1}) & if\ f(\boldsymbol{x}_{i2}) < f(\boldsymbol{x}_{i1}) \end{cases} \qquad \text{Eq. 14}$$

where $\boldsymbol{x}^i$ = the i-th individual in the population
$\boldsymbol{x}_{\text{teacher}}$ = the best individual
$\boldsymbol{x}_{\text{mean}}$ = mean values of other members in the population
rand = a uniform random number in the range of [0, 1]
T_F = teaching factor, which can be either 1 or 2 at random.
$\boldsymbol{x}_{i1}$ and $\boldsymbol{x}_{i2}$ = two randomly selected individuals in the population.

SATLBO-AP is the modification specifically adjusting for the parameter estimation type of problem. The change is done both in the teaching and learning phases of the algorithm. Multiple teachers are assigned in the teacher phase in order to avoid a premature convergence, while a three-student learning scheme is added to the learner phase. In the teaching phase diversity archive balancing is adopted between exploration and exploitation presented as:

$$\boldsymbol{x}_{teacher} = \begin{cases} \boldsymbol{x}_{best} & if\ rand < p_T \\ \boldsymbol{x}_{D,rand} & otherwise \end{cases} \qquad \text{Eq. 15}$$

where p_T is the probability of selecting the best solution, $rand \in [0,1]$ is a uniform random number, while $\boldsymbol{x}_{D,rand}$ is an individual randomly selected in the diversity archive. The teaching probability p_T can be defined in intervals, for example 3 intervals [0.4, 0.5], [0.5, 0.6] and [0.6, 0.7], where selection of the intervals is carried out using a roulette wheel selection technique with the probability of being selected as p_{wj}, which can be computed from Eq.16. For example, if subinterval one is selected, the value of p_T is generated as $p_T = 0.4 + rand(0.5 - 0.4)$.

$$p_{wj} = \frac{p_{T_{success},j}}{p_{T_{success},j}+p_{T_{fail},j}} \quad \text{Eq. 16}$$

The acceptance probability is added to prevent local optimum traps in p_{wj}. The updating scheme for both $p_{T\_success,j}$ and $p_{T\_fail,j}$ can be expressed as:

If $f(\boldsymbol{x}^i_{teaching}) \leq f(\boldsymbol{x}^i)$ Eq. 17

$p_{T\_success,j} = p_{T\_success,j} + 1$

Else

If $rand < p_{acc}$

$p_{T\_success,j} = p_{T\_success,j} + 0.5$

Else

$p_{T\_fail,j} = p_{T\_fail,j} + 1$

where p_{acc} is an acceptance probability set with a high value initially and reduced as the optimization run progresses. Although it failed, the $p_{T\_success,j}$ still has a chance to increase its score to 0.5 if the acceptance probability is passed. p_{acc} can be adjusted in this work, with the scheduling as displayed in Figure 2.

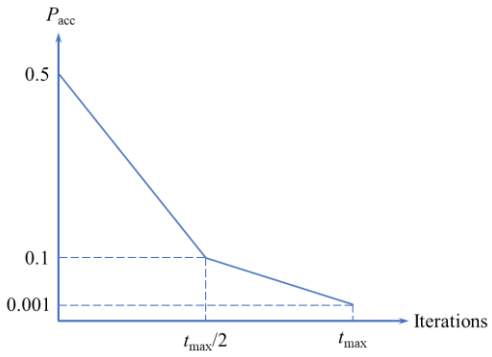

Figure 2 Acceptance probability scheduling

In the learning phase a three-student learning scheme is used alongside Eq.14 as in Eq 17, while p_L can be calculated like p_T in the teaching phase.

$$\boldsymbol{x}^i_{learner} = \begin{cases} Eq.14 & if\ rand < p_L \\ \boldsymbol{x}^i + rand(\boldsymbol{x}_{i3} - \boldsymbol{x}_{i1}) + rand(\boldsymbol{x}_{i3} - \boldsymbol{x}_{i2}) & otherwise \end{cases} \quad \text{Eq. 18}$$

where $\boldsymbol{x}_{i1}$, $\boldsymbol{x}_{i2}$, $\boldsymbol{x}_{i3}$ are randomly selected from the current population and the last one is the best of them. The procedure of SATLBO-AP starts with initializing a population, acceptance probability scheduling (p_{acc}), and initial sets of teaching and learning proverbiality $\boldsymbol{p}_{T\_success}$, $\boldsymbol{p}_{T\_fail}$ $\boldsymbol{p}_{L\_success}$, $\boldsymbol{p}_{L\_fail}$, evaluating the population and creating the diversity archive. Then, proceed to teaching and learning phases and update $\boldsymbol{p}_{T\_success}$, $\boldsymbol{p}_{T\_fail}$ $\boldsymbol{p}_{L\_success}$, $\boldsymbol{p}_{L\_fail}$ and p_{acc}. The search continues until the termination criterion is met. More details are given in Algorithm 1.

Algorithm 1 SATLBO-AP

Input: Maximum iteration number (*maxiter*), population size (n_P).
Output: $\boldsymbol{x}_{best}$, f_{best}
Main algorithm
1. Initialize a set of populations, $p_{L\_success,j}$, $p_{T\_success}$, p_{T_fail}, $p_{L\_fail,j}$, and p_{acc}
2. For i=1 to *maxiter*
  2.1 Identify the best solution, $\boldsymbol{x}_{best}$, f_{best}, and define $\boldsymbol{x}_{teacher} = \boldsymbol{x}_{best}$.
  (Teacher Phase)
  For j=1 to n_p
    2.2 Generate p_T based on $p_{T\_success,j}$, $p_{T\_fail,j}$.
    2.3 Update the population using Eq. (13) based on the $\boldsymbol{x}_{teacher}$ from Eq. (15)
      2.2.1 Evaluate the objective function value.
      2.2.2 Perform greedy selection.
      2.2.3 Update $p_{T\_success,j}$, $p_{T\_fail,j}$ using Eq. (17)
  End
  (Learner Phase)
  For j=1 to n_p
    2.4 Generate p_L based on $p_{L\_success,j}$, $p_{L\_fail,j}$.
    2.5 Update the population using Eq. (18)
      2.5.1 Evaluate the objective function value.
      2.5.2 Perform greedy selection.
      2.5.3 Update $p_{L\_success,j}$, $p_{L\_fail,j}$ based on Eq. (17).
  End
  Update p_{acc}
3. End

Full details of SATLBO-AP can be found in previous work [26].

5. Numerical experiment

A comparative study has been constructed to observe the performance of SATLBO-AP in lateral parameter estimation compared to a recently developed algorithm. The real flight data captured from the known coefficient, as in Figure 1, was then augmented with noise 0%, 5% and 10% in a total of 3 tested cases. The noise is determined by the percentage of the maximum amplitude of each signal, which then adds up to the signal. The MHs used in this study include:

Ant Lion Optimizer (ALO) [27],
Grasshopper Optimization Algorithm (GOA) [29],
Dragonfly Algorithm (DA) [28],
Grey Wolf Optimization (GWO) [30],
Moth-Flame Optimization Algorithm (MFO) [31],
Multi-Verse Optimizer (MVO) [32],
Sine Cosine Algorithm (SCA) [33],
Salp Swarm Algorithm (SSA) [34],
Water Cycle Algorithm (WCA) [35],
Whale Optimization Algorithm (WOA) [36],
Self-Adaptive Differential Evolution (SaDE) [37],
Improved Multi-Operator Differential Evolution (IMODE) [38],
Teaching-Learning Based Optimization [23],
Improved Teaching-Learning Based Optimization [25] and
Self-Adaptive Teaching-Learning Based Optimization with An Acceptance Probability (SaTLBO-AP) [26].

Each algorithm is used to solve the problems for 20 independent runs. The population size and maximum number of iterations are set to be 200 and 250, respectively. For any algorithm using a different population size, they will be terminated at the same number of function evaluations (FEs) of 200x250 = 50,000 FEs. The worst, best and average fitness values of all the runs are captured for comparison, together with the Friedman test. The Friedman test is a non-parametric statistic that can identify how the members of the group are significantly different from each other, and then rank the members from worst to best, so lower is better.

6. Results and discussion

The performances of 15 algorithms were evaluated across three scenarios: data without noise, data with 5% noise, and data with 10% noise. Among the algorithms tested, SATLBO-AP consistently outperforms a recently developed competitor, demonstrating superior performance in terms of Friedman ranking and mean fitness value, with low standard deviation and high consistency, as shown in Table 3. The runner-up, IMODE, also performs exceptionally well, particularly in terms of its minimum fitness value across all 20 independent runs. In cases of no noise and 10% noise added, IMODE achieved the lowest minimum fitness value compared to the other algorithms. In the 5% noise case, SATLBO-AP had a slightly lower fitness value. However, IMODE's worst solution (the highest fitness value) is still larger than that of SATLBO-AP by a noticeable margin, although this gap narrows as noise levels increase. Interestingly, the standard deviation for SCA is the lowest in all experimental cases, significantly lower than all other algorithms, including SATLBO-AP. Nevertheless, the fitness values are excessive. GWO shows good average fitness, but its standard deviation is higher than that of SSA, which ranked fourth. Although MFO, TLBO, and ITLBO rank very close to each other, the optimal points of TLBO and ITLBO are noticeably spread from MFO, indicated by the worst fitness, the best fitness and standard deviation in all three cases. Only in the first case of TLBO is the discrepancy minimal. WCA's average value is comparable to or even better than SSA and ALO, whereas the ranking is higher, because it only managed to find the optimal result half of the time. The feasibility of the result is classified when the value does not exceed 30; if it is, the run will be considered as infeasible, and that solution is classified as not a number (NaN). It is not involved in the result calculation as the data will misinform the overall performance. Though the number of feasible runs of WCA and GOA are very similar, the performance of WCA is better. The range of optimal design variables is enlarged by increasing the noise level in the validation data. The fitness value is certainly increasing according to noise level, thus the lower fitness value indicates an improvement in the search performance, as evidenced by DA, MFO, MVO, WCA and ITLBO. The mean fitness value of these algorithms when 5% noise was added is lower than that with no additional noise at all.

Table 3 Best, worst, average, standard deviation and Friedman test at 50,000 function evaluations of 20 individual runs from 15 algorithms, with and without added noise

Algorithms	Without noise						Noise 5%						Noise 10%					
	Worst	**Best**	**Mean**	**Std**	**FR**	**FS**	**Worst**	**Best**	**Mean**	**Std**	**FR**	**FS**	**Worst**	**Best**	**Mean**	**Std**	**FR**	**FS**
ALO	7.1424	0.8888	2.6014	1.3109	5.6	20	4.7692	1.1579	2.6674	1.0675	6.3	20	6.0674	1.5078	3.0962	0.9435	6.7	20
DA	23.8578	3.4449	7.1207	5.6971	10.7	20	12.4659	2.8689	4.9523	2.4255	10.2	19	13.7471	3.2114	5.081	2.7332	10.25	20
GOA	17.5355	4.4403	10.3147	5.5101	12.7	9	24.4663	4.4526	14.8514	6.6985	12.9	13	29.8595	5.3884	17.2299	9.1710	13.35	10
GWO	3.2524	0.5338	1.4785	0.9698	3.3	20	3.3751	0.8312	1.6363	0.8505	3.1	20	3.4084	1.4652	2.1593	0.6107	3.15	20
MFO	4.2307	1.9054	3.2441	0.5124	7.5	20	3.6557	1.9972	3.1224	0.4187	7.4	20	3.7703	2.2875	3.2067	0.4141	7.35	20
MVO	NaN	NaN	NaN	NaN	14.6	0	27.0484	10.5140	18.7812	11.6916	14.4	2	16.2825	11.5028	13.8927	3.3797	14.55	2
SCA	3.5340	3.2266	3.4440	**0.0748**	8.3	20	3.6493	3.0699	3.4459	**0.1338**	8.8	20	3.5813	3.2443	3.5141	**0.0941**	8.8	20
SSA	3.5376	0.8822	2.2238	0.5730	4.9	20	3.6238	1.1939	2.3970	0.6467	5.4	20	3.3503	1.8520	2.5829	0.4082	4.65	20
WCA	3.4182	1.8241	2.4376	0.5739	10.6	9	3.4865	0.7735	2.2536	0.8545	10.9	8	4.3154	2.1295	2.7773	0.6085	9.225	12
WOA	21.2302	2.2325	6.2794	4.7273	9.6	20	16.6958	1.8023	6.6637	4.4059	10.2	20	19.3455	3.1856	7.7167	5.8064	11.25	18
SADE	27.7137	5.7695	12.7049	5.789	12.3	18	28.1223	3.4217	13.4939	7.7028	12.4	18	21.0771	7.6126	12.8534	4.1188	12.475	18
IMODE	2.5519	**0.0584**	1.0161	0.7777	2.2	20	2.1680	0.6481	1.2929	0.5757	2.3	20	2.4048	**1.4090**	2.0025	0.3761	2.3	20
TLBO	3.7330	1.8025	2.8393	0.6204	7.3	19	23.6885	2.2359	4.0865	4.7675	7.1	19	9.8423	2.1322	3.3660	1.5887	7.05	20
ITLBO	23.1787	1.7941	6.7517	7.1997	8.8	17	13.0576	1.9739	3.6257	2.9871	7.2	19	25.2085	2.3085	4.2444	5.1843	7.2	19
SATLBO-AP	**1.9104**	0.1181	**0.7439**	0.5621	1.7	20	**1.5405**	**0.6462**	**1.0653**	0.3250	1.9	20	**2.3294**	1.4254	**1.7510**	0.2781	1.7	20

*FR is the Friedman test ranking; lower is better
**FS is the number of feasible runs

Figure 3 shows the top 4 algorithms' average fitness over 20 individual runs, in which at the beginning of the search, GWO and IMODE are converging rapidly and get trapped at around 20000 to 30000 Fes, while SATLBO-AP is still reaching the optimal solution. The reproduction strategy plays a key role in determining the exploration and exploitation balance of an algorithm. In GWO, the top three best solutions are selected as the alpha, beta and delta wolves to guide the search agent to the optimal solution. In contrast, both SATLBO-AP and IMODE employ more diverse reproduction strategies and incorporate an archive as the updating population, which helps prevent premature convergence. Typically, selecting the best solution in each iteration will lead to fast convergence, but reduced population diversity. The SATLBO-AP convergence rate is relatively slow compared to IMODE due to the acceptance probability approach, which prevents the SATLBO's adaptive parameters from quickly adapting to the local optimal value. But in end it continues converging nearer the global optimal point than other algorithms. Both SaDE and IMODE also utilize self-adaptive approaches. SaDE in previous work is very effective in parameter estimation on longitudinal problems in second place. In this problem however, it performs poorly, which indicates how different this problem is compared to the longitudinal one that has fewer design variables, resulting in an exponentially larger search space, making the problem harder to solve. IMODE on the other hand performs exceptionally well. When compared to the results of TLBO's family, SATLBO-AP performs significantly better in terms of both exploration and exploitation, as suggested in Table 3 and Figure 4. Moreover, it succeeds in searching every time, unlike other variations that occasionally fail to find the optimal solution.

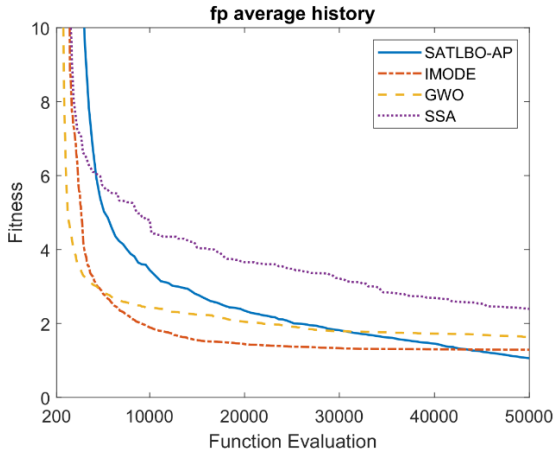

Figure 3 The average fitness value of 20 runs from the top 4 best algorithms in this experiment for data without noise.

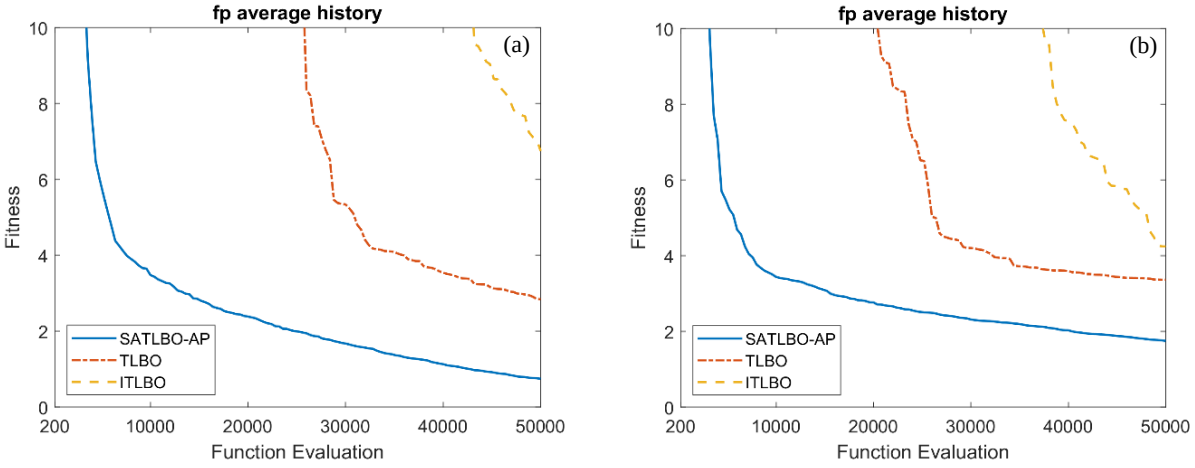

Figure 4 The average fitness value of 20 runs from TLBO family for data (a) without noise and (b) added noise at 10%

The coefficient obtained from the optimal result and the real coefficient, as shown in Figure 5, are relatively close to each other even when 10% noise is present. The dashed red line is the real coefficient, the solid black line is the coefficient obtained from the SATLBO-AP, and the blue line is the data used as a reference to the optimization algorithm. In around 10 to 14 seconds of simulation, the noise level is very high relative to the real signal, which potentially misleads the optimal result. Fortunately, there are 6 outputs used to calculate the objective function; with more responsive signal shapes the optimal result is as it should be.

7. Conclusion

The SATLBO-AP has been tested in aircraft parameter estimation for both longitudinal and lateral dynamics and it is the best compared to recently developed algorithms. It outperforms others in terms of performance and consistency. Although at the start the convergence rate is low compared to GWO and IMODE due to the adaptive strategy and acceptance probability combined, in the long run, the algorithm adapts to the problem, leading to a performance increase in the second half which continues converging. The parameter acquired by the optimization is very accurate even when adding noise to the data. The trend of the identified system is nearly identical to the validation data, and can be improved simply by increasing the function evaluation, or in other words iterations. SATBLO-AP is not only good for aircraft longitudinal dynamic identification but also for lateral dynamics.

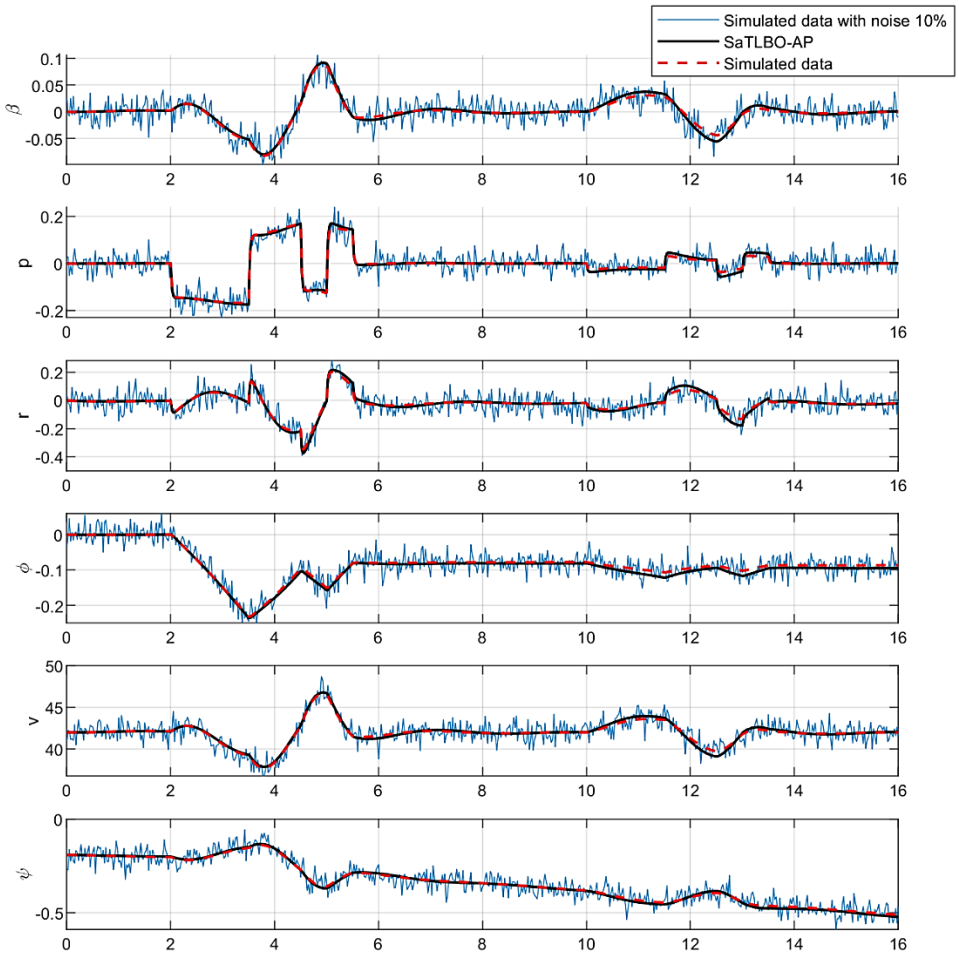

Figure 5 The best result of SaTLBO-AP compared to the real coefficient simulated with noise at 10%

8. Acknowledgement

The authors are grateful for financial support by the National Research Council of Thailand, Grant No. N42A650549.

9. References

[1] Blake WB. Prediction of fighter aircraft dynamic derivatives using Digital Datcom. AIAA 3rd Applied Aerodynamics Conference; 1985 Oct 14-16; Colorado, United States. New York: AIAA; 1985. p. 1-8.
[2] Drela M, Youngren H. Athena vortex lattice (AVL). Computer software AVL [Internet]. 2008 [cited 2024 Sep 28]. Available from: https://web.mit.edu/drela/Public/web/avl/.
[3] Wendt JF. Computational fluid dynamics. 3rd ed. Berlin: Springer; 2009.
[4] Peyada NK, Sen A, Ghosh AK. Aerodynamic characterization of HANSA-3 aircraft using equation error, maximum likelihood and filter error methods. Proceedings of the International MultiConference of Engineers and Computer Scientists 2008 Vol IIIMECS 2008; 2008 Mar 19-21; Hong Kong. Hong Kong: IAENG; 2008. p. 1-6.
[5] Morelli EA. Practical aspects of the equation-error method for aircraft parameter estimation. AIAA Atmospheric Flight Mechanics Conference; 2006 Aug 21-24; Keystone, United States. Virginia: AIAA; 2006. p. 1-18.
[6] Olkkonen JT, Olkkonen H. Least squares matrix algorithm for state-space modelling of dynamic systems. J Signal Inf Process. 2011;2(4):287-91.
[7] Kamali C, Pashilkar AA, Raol JR. Evaluation of recursive least squares algorithm for parameter estimation in aircraft real time applications. Aerosp Sci Technol. 2011;15(3):165-74.
[8] Jategaonkar RV, Plaetschke E. Algorithms for aircraft parameter estimation accounting for process and measurement noise. J Aircr. 1989;26(4):360-72.
[9] Góes LCS, Hemerly EM, De Oliveira MacIel BC, Neto WR, Mendonca CB, Hoff J. Aircraft parameter estimation using output-error methods. Inverse Probl Sci Eng. 2006;14(6):651-64.
[10] Grauer JA, Boucher MJ. Identification of aeroelastic models for the X-56A longitudinal dynamics using multisine inputs and output error in the frequency domain. Aerospace. 2019;6(2):24.
[11] Majeed M, Singh J. Frequency and time domain recursive parameter estimation for a flexible aircraft. IFAC Proc Vol. 2013;46(19):453-8.
[12] Campbell ME, Brunke S. Nonlinear estimation of aircraft models for on-line control customization. 2001 IEEE Aerospace Conference Proceedings; 2001 Mar 10-17; Big Sky, USA. USA: IEEE; 2001. p. 621-8.

[13] Kallapur AG, Anavatti SG. UAV linear and nonlinear estimation using extended Kalman filter. 2006 International Conference on Computational Inteligence for Modelling Control and Automation and International Conference on Intelligent Agents Web Technologies and International Commerce (CIMCA'06); 2006 Nov 28 – Dec 1; Sydney, Australia. USA: IEEE; 2006. p. 1-5.
[14] Chowdhary G, Jategaonkar R. Aerodynamic parameter estimation from flight data applying extended and unscented Kalman filter. Aerosp Sci Technol. 2010;14(2):106-17.
[15] Singh S, Ghosh AK. Estimation of lateral-directional parameters using neural networks based modified delta method. Aeronaut J. 2007;111(1124):659-67.
[16] Raisinghani SC, Ghosh AK. Parameter estimation of an aeroelastic aircraft using neural networks. Sadhana. 2000;25(2):181-91.
[17] Peyada NK, Ghosh AK. Aerodynamic parameter estimation using new filtering technique based on neural network and gauss-newton method. 6th National Seminar on Aerospace & Related Mechanisms (ARMS 2008); 2008 Mar 28-29; Pune, India. Pune: ARDE; 2008. p. 243-52.
[18] Li X, Yin M. Parameter estimation for chaotic systems by hybrid differential evolution algorithm and artificial bee colony algorithm. Nonlinear Dyn. 2014;77(1-2):61-71.
[19] Ghosh Roy A, Peyada NK. Aircraft parameter estimation using Hybrid Neuro Fuzzy and Artificial Bee Colony optimization (HNFABC) algorithm. Aerosp Sci Technol. 2017;71:772-82.
[20] Sun J, Garibaldi JM, Hodgman C. Parameter estimation using metaheuristics in systems biology: a comprehensive review. IEEE/ACM Trans Comput Biol Bioinform. 2012;9(1):185-202.
[21] Jiang H, Wang J, Wu J, Geng W. Comparison of numerical methods and metaheuristic optimization algorithms for estimating parameters for wind energy potential assessment in low wind regions. Renew Sustain Energy Rev. 2017;69:1199-217.
[22] Çanakoğlu AI, Yetgin AG, Temurtaş H, Turan M. Induction motor parameter estimation using metaheuristic methods. Turk J Electr Eng Comput Sci. 2014;22(5):1177-92.
[23] Rao RV, Savsani VJ, Vakharia DP. Teaching-learning-based optimization: a novel method for constrained mechanical design optimization problems. CAD Comput Aided Des. 2011;43(3):303-15.
[24] Wichapong K, Bureerat S, Pholdee N. Solving inverse kinematics of robot manipulators by means of meta-heuristic optimisation. IOP Conf Ser Mater Sci Eng. 2018;370(1):012056.
[25] Li S, Gong W, Yan X, Hu C, Bai D, Wang L, et al. Parameter extraction of photovoltaic models using an improved teaching-learning-based optimization. Energy Convers Manag. 2019;186:293-305.
[26] Kanokmedhakul Y, Panagant N, Bureerat S, Pholdee N, Yildiz AR. Aircraft control parameter estimation using self-adaptive teaching-learning-based optimization with an acceptance probability. Comput Intell Neurosci. 2021;2021:4740995.
[27] Mirjalili S. The ant lion optimizer. Adv Eng Softw. 2015;83:80-98.
[28] Mirjalili S. Dragonfly algorithm: a new meta-heuristic optimization technique for solving single-objective, discrete, and multi-objective problems. Neural Comput Appl. 2016;27(4):1053-73.
[29] Saremi S, Mirjalili S, Lewis A. Grasshopper optimisation algorithm: theory and application. Adv Eng Softw. 2017;105:30-47.
[30] Mirjalili S, Mirjalili SM, Lewis A. Grey wolf optimizer. Adv Eng Softw. 2014;69:46-61.
[31] Mirjalili S. Moth-flame optimization algorithm: a novel nature-inspired heuristic paradigm. Knowledge-Based Syst. 2015;89: 228-49.
[32] Mirjalili S, Mirjalili SM, Hatamlou A. Multi-verse optimizer: a nature-inspired algorithm for global optimization. Neural Comput Appl. 2016;27(2):495-513.
[33] Mirjalili S. SCA: a sine cosine algorithm for solving optimization problems. Knowledge-Based Syst. 2016;96:120-33.
[34] Mirjalili S, Gandomi AH, Mirjalili SZ, Saremi S, Faris H, Mirjalili SM. Salp swarm algorithm: a bio-inspired optimizer for engineering design problems. Adv Eng Softw. 2017;114:163-91.
[35] Eskandar H, Sadollah A, Bahreininejad A, Hamdi M. Water cycle algorithm - a novel metaheuristic optimization method for solving constrained engineering optimization problems. Comput Struct. 2012;110-111:151-66.
[36] Mirjalili S, Lewis A. The whale optimization algorithm. Adv Eng Softw. 2016;95:51-67.
[37] Qin AK, Suganthan PN. Self-adaptive differential evolution algorithm for numerical optimization. 2005 IEEE congress on evolutionary computation; 2005 Sep 2-5; Edinburgh, UK. USA: IEEE; 2005. p. 1785-91.
[38] Sallam KM, Elsayed SM, Chakrabortty RK, Ryan MJ. Improved multi-operator differential evolution algorithm for solving unconstrained problems. 2020 IEEE Congress on Evolutionary Computation (CEC); 2020 Jul 19-24; Glasgow, UK. USA: IEEE; 2020. p. 1-8.
[39] Bureerat S, Sleesongsom S. Constraint handling technique for four-bar linkage path generation using self-adaptive teaching–learning-based optimization with a diversity archive. Eng Optim. 2020;53(3):513-30.
[40] Bureerat S, Pholdee N. Inverse problem based differential evolution for efficient structural health monitoring of trusses. Appl Soft Comput. 2018;66:462-72.
[41] Sleesongsom S, Bureerat S. Four-bar linkage path generation through self-adaptive population size teaching-learning based optimization. Knowledge-Based Syst. 2017;135:180-91.